Impurity Clustering and Ferromagnetic Interactions that are not Carrier Induced in Dilute Magnetic Semiconductors: The Case of Cu_2O:Co

Hannes Raebiger, Stephan Lany, and Alex Zunger

National Renewable Energy Laboratory, Golden, Colorado 80401, USA

Current models for ferromagnetism in diluted magnetic semiconductors, such as ''p-d exchange'' or ''double-exchange'', rely on the presence of partially filled gap states. We point out a new mechanism, not requiring partially filled states, in which ferromagnetic coupling arises from the occupation of previously unoccupied levels when two transition metal impurities form a close pair. We find from first-principles calculations that this mechanism explains strong ferromagnetic coupling between Co impurities in Cu_2O, and at the same time gives rise to Co clustering.

Nonmagnetic semiconductors (GaAs, ZnTe) can be made ferromagnetic by doping via ~1% of substitutional magnetic ions (e.g., V, Cr, and Mn), leading to the interesting situation where magnetism is controlled via the density of free carriers (electrons or holes) in the sample [1–3]. Despite early attempts at RKKY-descriptions involving the picture of a delocalized hole [4,5] or a polaron [6,7] leading to magnetic coupling, the picture that now emerges is simpler [8–11]: The substitutional impurity [denoted TM in Fig. 1(a)] introduces inside the band gap a partially occupied level. There is an energy gain when two such levels [TM-TM in Fig. 1(a)] couple ferromagnetically [9,10], because the lower energy bonding state is occupied preferentially. This simple picture underlies the qualitative models for ''p-d exchange'' and ''double exchange,'' and explains the predicted [9,11] and verified [12] *orientation* dependence of the interaction in terms of the shapes of the interacting orbitals (e or t_2) and the ability to control, i.e., enhance [11,13] or eliminate [11,14] magnetism when the Fermi level is shifted via doping or defects. Another qualitative model is ''superexchange'' (exchange over ligand atoms), which, however, usually leads to antiferromagnetic coupling. Only under special conditions superexchange may cause weak ferromagnetic interactions [15], which are unlikely to stabilize ferromagnetism in dilute systems (see Ref. [16]).

A different mechanism for ferromagnetic pair-interaction which does not require partially filled levels is illustrated in Fig. 1(b) for the fully occupied (closed shell) $e^2 t^0$ configuration on each TM site: If the interaction between two TM impurities were strong enough (so that the e_g-derived antibonding level would rise above the t_2-derived bonding level) then the electrons of the coupled system would drop into the previously unoccupied t_2-derived bonding state, thereby gaining energy and stabilizing the ferromagnetic configuration. However, this type of magnetic pair-interaction has so far not been identified, probably because of the generally small e(TM)-e(TM) interaction between two e_g levels in the

zinc-blende structure [11], and because of the rather large t_2-e_g crystal-field splitting (~1 eV [9]) in typical host crystals such as GaAs.

Cu_2O has the simple and highly symmetric cuprite structure (space group O_h) with six atoms in the unit cell, shown in Fig. 2, and serves as a prototype for understanding ferromagnetism in other oxides. We show here from first-principles total-energy calculations that Co impurities in Cu_2O exhibit strong ferromagnetic pair-interaction despite the absence of partially occupied levels for the isolated Co_{Cu} impurity. The origin of ferromagnetism in Cu_2O:Co lies in the occupation of previously unoccupied levels, analogous to the case illustrated in Fig. 1(b). Thus, our model provides a basis to explain ferromagnetism which is not carrier-mediated, as it has indeed been noted experimentally for the Cu_2O:Co system [17]. Furthermore, the magnetic TM-TM coupling provides a driving force for impurity clustering. Such clusters may exhibit internally strong ferromagnetic interaction and weaker long-range interaction like Mn clusters in GaAs:Mn [18,19]. Ultimately, the clustering may lead to a spinodal decomposition and an ensuing high Curie temperature [20].

Method.—Total energies and electronic structures are calculated within the generalized gradient approximation (GGA-PBE) to density-functional theory using the projec-
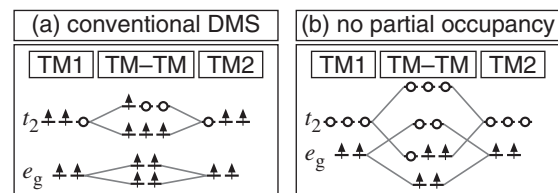
FIG. 1. Schematic energy level coupling diagram for the ferromagnetic interaction of transition metal TM pair in (a) conventional diluted magnetic semiconductor case [9–11], and (b) in a system with no partially filled levels. Here empty circles denote unoccupied levels.
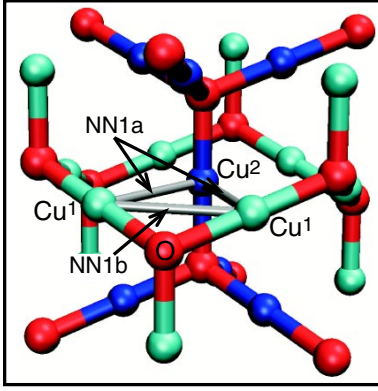
FIG. 2 (color online). The cuprite structure, which consists of two interpenetrating cristobalite lattices. The blue and cyan spheres represent Cu atoms in the separate cristobalite lattices labeled Cu^1 and Cu^2, while red spheres represent the O atoms. The gray lines indicate nearest neighbor Cu-Cu bonds either connecting the two (NN1b) cristobalite lattices or within one (NN1a).

tor augmented-wave method as implemented in the VASP code [21]. Plane waves are included up to the cut-off energy of 400 eV. Doped and pure Cu_2O are modeled in supercells consisting of 96 atoms using lattice constant for pure Cu_2O of 4.313 Å calculated within GGA-PBE, and allowing all atomic positions to relax. For total energies a $\vec{k}$-point mesh of $4 \times 4 \times 4$ including the Γ-point is used, while structural relaxations are performed with fewer $\vec{k}$ points.

We calculate defect formation energies $\Delta H_{D,q}$ for defect D in charge state q as a function of Fermi energy ε_F and chemical potential μ as

$$\Delta H_{D,q}(\varepsilon_F, \mu) = (E_{D,q} - E_H) + \sum_\alpha n_\alpha \mu_\alpha + q\varepsilon_F. \quad (1)$$

Here E_H is the total energy of the pure host, and $E_{D,q}$ that of a system with defect(s). $\mu_\alpha = \mu_\alpha^{elem} + \Delta\mu_\alpha$ is the chemical potential of a reservoir of atoms α, and n_α is $+1$ or -1 for atoms added to the reservoir or removed from it, respectively. The reference chemical potential μ_α^{elem} for metal elements is taken as that of the solid metal, and for oxygen as that of the O_2 molecule. $\Delta\mu_{Cu}$ and $\Delta\mu_O$ are determined by the condition of maintaining thermodynamic equilibrium with Cu_2O and either CuO (O-rich/Cu-poor) or Cu-metal (O-poor/Cu-rich), as described in Ref. [22]. We describe the O-poor/Cu-rich growth conditions with $\Delta\mu_{Cu} = 0$ and $\Delta\mu_O = -1.26$ eV [22], and the O-rich/Cu-poor conditions with $\Delta\mu_{Cu} = -0.16$ and $\Delta\mu_O = -0.93$ eV [22]. The last term in Eq. (1) is the energy of free carriers of charge q at Fermi energy ε_F, which varies between valence band maximum (VBM) and conduction band minimum (CBM). The defect energies $E_{D,q}$ are corrected for band gap error [23], band filling, and image charges in the finite supercell method together with proper potential alignment, as described in

Ref. [24]. Transition levels $\varepsilon(q, q')$, i.e., the ionization energy from charge q to q' are evaluated as the value of ε_F at which $\Delta H_{D,q}$ and $\Delta H_{D,q'}$ intersect.

The stable charge state of Co_{Cu}.—The formation energy of a single Co_{Cu} is shown in Fig. 3. Co_{Cu} has a single donor transition level $\varepsilon(+/0)$ at VBM + 0.26, and single and double acceptor transition levels at $\varepsilon(0/-) = $ VBM + 1.10 and $\varepsilon(-/2-) = $ VBM + 1.58 eV, respectively. To determine the stable charge state of Co_{Cu} in Cu_2O we must recognize that even the pure host material is never stoichiometric and has, at given growth temperature, a concentration of free carriers that are going to determine the electronic and magnetic configuration of substitutional Co_{Cu}. We have previously found [22] that the dominant intrinsic defect is the V_{Cu} acceptor (Fig. 3) that renders Cu_2O cation deficient and p type. We follow the same procedure as in Ref. [25] to determine the equilibrium Fermi level in the presence of both intrinsic defects [22] and intentional Co doping in Cu_2O. For a Co concentration of 5% (i.e., 5% of Cu sites substituted by Co) and a growth temperature [17] of $T = 700\,°C$ we find that the equilibrium Fermi level (at room temperature) is between VBM + 0.32 eV (under O-rich/Cu-poor conditions) and VBM + 0.34 eV (under O-poor/Cu-rich conditions). At this Fermi level the substitutional Co_{Cu} (see Fig. 3) is almost exclusively in the charge neutral state Co_{Cu}^0, for which we determine the electronic structure and magnetic interactions in the following.

Single substitutional Co_{Cu} *has a magnetic moment, but no partially filled levels.*—In the cation site symmetry D_{3d} the d levels split into two e_g and one a_{1g} levels, of which the fully occupied majority spin $(+)$ levels $e_{g+}^2 a_{1g+}^1 e_{g+}^2$ are resonant in the valence band [26]. The minority spin $(-)$ density of states of the Co d levels (split by ~ 2 eV from the majority spin levels) is shown in Fig. 4(a). Here the e_{g-} level below the VBM and the a_{1g-} level in the gap are fully occupied, while the e_{g-} level in the gap is empty. Based on our calculated density of states, we give the single-particle level occupation scheme in Fig. 4(b). This occupation $(e_{g+}^2 a_{1g+}^1 e_{g+}^2 e_{g-}^2 e_{g-}^1 e_{g-}^0)$ leads to a net magnetization of
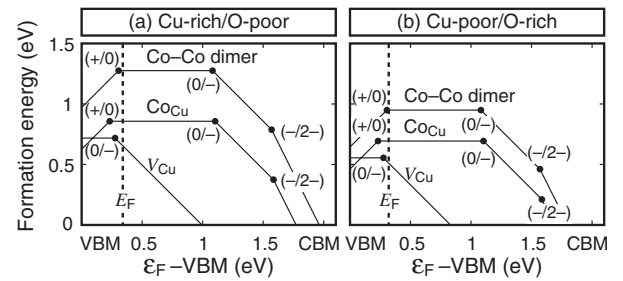
FIG. 3. (a) Formation energies, Eq. (1), of V_{Cu}, Co_{Cu}, and Co_{Cu}-Co_{Cu} in Cu-rich/O-poor conditions; and (b) in Cu-poor/O-rich conditions as a function of Fermi energy ε_F. The solid dots denote the transition levels $\varepsilon(q, q')$. The equilibrium Fermi level E_F is calculated for a Co concentration of 5%.

2 Bohr magnetons per Co atom, but as none of the levels are partially filled, Cu_2O:Co is not expected to be ferromagnetic within the conventional carrier-mediated mechanism of Fig. 1(a).

Strong interaction and level splitting within the Co-Co *dimer in the cuprite lattice*.—In the cuprite structure (Fig. 2) that consists of two interpenetrating cristobalite lattices it is possible to form two different nearest neighbor cation pairs that, on the ideal lattice, have equal distances: the NN1a pair Cu^1-Cu^2 that connects two cristobalite lattices; and the NN1b pair Cu^1-Cu^1 within a single cristobalite sublattice that forms a Cu^1-O-Cu^1 chain. For the NN1a pair the level splitting due to magnetic TM-TM interaction (''interaction splitting'') is large compared with the crystal-field splitting, as seen in the Co-d minority spin density of states given in Fig. 4(c). From charge density analysis (not shown) we identify the peaks seen in Fig. 4(c) above VBM as being bonding (e^b) and antibonding (e^a) Co-d levels. Figure 4(d) shows schematically the rearrangement of the Co minority spin d levels in response to dimer formation. We see that the bonding levels formed from the e_g levels (unoccupied for the isolated Co_{Cu}) lie lower in energy than the antibonding levels formed from the e_g levels (occupied for the isolated Co_{Cu}). Hence, the electrons will relax into the lower energy bonding levels, yielding an energy gain from ferromagnetic coupling in NN1a, as illustrated in Fig. 1(b). Because of this electron transfer from antibonding to bonding levels, the Co atoms move towards each other, forming a compact dimer with a very short Co-Co bond distance of

FIG. 4 (color online). (a) Calculated Co-d orbital projected density of states of single substitutional Co_{Cu}; and (b) schematic majority and minority spin single-particle energy levels for Co_{Cu} in D_{3d} symmetry. (c) Calculated Co-d orbital projected density of states of Co-Co NN1a dimer; and (d) schematic bonding scheme for minority spin Co_{Cu}-Co_{Cu} dimer in NN1a geometry in D_2 symmetry. Occupied bonding (unoccupied antibonding) levels formed from unoccupied (occupied) e_g levels of the isolated Co_{Cu} are shown in red (blue).

2.23 Å. This dimer bond length is significantly shorter than the Cu-Cu distance in Cu_2O of 3.05 Å, and even shorter than the Co-Co distance of 2.51 Å in bulk hcp Co. The energy gain due to the level interaction shown in Fig. 4(d) requires ferromagnetic alignment between the two Co impurities. In the antiferromagnetic configuration, the majority spin direction of one Co interacts with the minority spin of the other Co. Because of the exchange splitting of ~2 eV, this interaction is much weaker, and no energy gain due to the occupation of previously unoccupied levels occurs. Contrary to the NN1a pair discussed above, in the NN1b pair (i.e., the Co-O-Co complex), the interaction splitting remains smaller than the crystal-field splitting and there is neither an energy gain nor a structural relaxation upon ferromagnetic coupling.

Ferromagnetic stabilization and pair binding energy resulting from the level rearrangement.—The total energy difference Δ_{FM} between ferromagnetic E_{FM} and antiparallel E_{AFM} spin alignment of the pair Co^1-Co^2 is defined as

$$\Delta_{FM} = E_{FM}[\text{Co-Co}] - E_{AFM}[\text{Co-Co}]. \qquad (2)$$

The binding energy E_b is the energy difference between a pair and two isolated impurities

$$E_b = \Delta H[\text{Co-Co}] - 2\Delta H[\text{Co}]. \qquad (3)$$

Aside the first nearest neighbor pairs (NN1a and NN1b), we also consider third nearest neighbor (NN3a and NN3b), and seventh nearest neighbor pairs (NN7b); here the ''a'' denotes that the Co atoms are in different cristobalite sublattices, and the ''b'' that both atoms are in one and the same cristobalite sublattice. All Co-Co pairs are ferromagnetic. The magnetic stabilization and binding energies for each pair are given in Table I. The strongest magnetic coupling is found for the NN1a pair, while for the other pairs the coupling is much weaker. No value of Δ_{FM} is given for the NN1b pair, because the antiferromagnetic configuration is unstable (only a nonmagnetic solution is obtained). As indicated by the respective binding energies, the NN1a pair is far more stable than the NN1b pair, so Co-Co NN pairs will almost exclusively exist in the NN1a configuration. Sieberer *et al.* who considered only the less stable NN1b pair for Co in Cu_2O, found that magnetism can be strongly influenced when lattice vacancies exist at very high concentrations (one vacancy per TM pair). In our thermodynamic simulations of the intrinsic defect concentrations in Cu_2O:Co, however, we found that lattice vacancies stay below $[V_{Cu}] = 1.2 \times 10^{20}$ cm^{-3} (0.25%) and $[V_O] = 3.5 \times 10^{18}$ cm^{-3} at a Co concentration of 5%.

TABLE I. Magnetic stabilization energy Δ_{FM} and binding energy E_b for various Co-Co pairs.

Pair	NN1a	NN1b	NN3a	NN3b	NN7b
Δ_{FM} (meV)	−441	⋯	−21	−1	−8
E_b (meV)	−439	−45	−27	−2	−8

The calculated binding energies practically equal the ferromagnetic stabilization energies, which is expected from the absence of magnetic interaction in the antiferromagnetic configuration, and the absence of electrostatic and elastic Co-Co interaction (Co_{Cu}^{0} is charge neutral and the isolated Co_{Cu} induces only marginal lattice relaxation). Since the calculated equilibrium Fermi level is very close to the NN1a $\varepsilon(+/0)$ transition level (shown in Fig. 3), we also calculate Δ_{FM} for the positively charged NN1a^{+}, and find an equally strong ferromagnetic coupling of $\Delta_{FM} = -438$ meV, as in the charge neutral NN1a dimer, thus confirming that indeed the magnetic pair-interaction is independent of carrier doping.

Strong dimer binding leads to formation of larger clusters.—To assess the possibility of formation of larger clusters, we calculate the binding energy of a third Co atom to the existing NN1a dimer as

$$E_b^{(3)} = \Delta H[\text{Co-Co-Co}] - \Delta H[\text{Co-Co}] - \Delta H[\text{Co}], \quad (4)$$

in neutral charge state. We obtain values of $E_b^{(3)} = 357$, 260, and -468 meV for a linear chain, a chain with 120°, and for a compact triangle cluster, respectively. Of these clusters, only the compact triangle cluster has a negative binding energy, i.e., is energetically favored. The chainlike clusters are energetically unfavorable because the middle Co_{Cu} can only relax towards one of the two other Co_{Cu} atoms, causing frustration. On the other hand, forming a compact triangular cluster the third atom is strongly bound to the initial dimer. Furthermore, the energy gain in forming the compact triangle from an NN1a pair plus an isolated Co_{Cu} is within meV accuracy the same as that in forming the NN1a pair from two Co_{Cu} atoms. This is because in the compact triangle another NN1a bond is formed. It is likely that even further Co atoms will attach to the cluster preferring compact geometries that allow formation of further NN1a bonds. Considering the fact that the copper vacancy has a low migration barrier of [27] 0.3 eV and assuming that V_{Cu} provides a vehicle for diffusion for Co_{Cu} (similarly as V_{Ga} for Mn_{Ga} in (Ga,Mn)As [28]), the Co_{Cu} may be mobile even in room temperature, which would lead to significant clustering. The clustering mechanism that arises from occupying levels that were unoccupied in the isolated impurity favors parallel spin alignment inside the cluster, and therefore each cluster carries a large magnetic moment. The strong intracluster magnetic order in turn is a prerequisite for high temperature magnetic order in a spinodal ferromagnet [20].

In summary, we propose that ferromagnetic pair interaction in a semiconductor can arise from occupying previously unoccupied levels in the presence of a large interaction splitting, in which case the coupling is independent of charge carriers and does not require partially occupied levels. We show that this kind of ferromagnetic coupling takes place in nearest neighbor Co-Co pairs in Cu_2O leading to the formation of compact, ferromagnetic Co clusters.

[1] H. Ohno, Science **281**, 951 (1998).
[2] H. Akinaga and H. Ohno, IEEE Trans. Nanotechnol. **1**, 19 (2002).
[3] T. Jungwirth *et al.*, Rev. Mod. Phys. **78**, 809 (2006).
[4] T. Dietl, H. Ohno, and F. Matsukura, Phys. Rev. B **63**, 195205 (2001).
[5] M. Abolfath *et al.*, Phys. Rev. B **63**, 054418 (2001).
[6] A. Kaminski and S. Das Sarma, Phys. Rev. Lett. **88**, 247202 (2002).
[7] J. M. D. Coey, M. Venkatesan, and C. B. Fitzgerald, Nat. Mater. **4**, 173 (2005).
[8] G. Alvarez and E. Dagotto, Phys. Rev. B **68**, 045202 (2003).
[9] P. Mahadevan, D. D. Sarma, and A. Zunger, Phys. Rev. Lett. **93**, 177201 (2004).
[10] P. Mahadevan and A. Zunger, Phys. Rev. B **69**, 115211 (2004).
[11] Y.-J. Zhao, P. Mahadevan, and A. Zunger, J. Appl. Phys. **98**, 113901 (2005).
[12] D. Kitchen *et al.*, Nature (London) **442**, 436 (2006).
[13] K.-T. Nam *et al.*, Phys. Status Solidi B **241**, 668 (2004).
[14] S. T. B. Goennenwein *et al.*, Phys. Rev. Lett. **92**, 227202 (2004).
[15] P. W. Anderson, in *Magnetism I*, edited by G. T. Rado and H. Suhl (Academic, New York, 1963).
[16] See EPAPS Document No. E-PRLTAO-99-050742 for supplementary material to this article. For more information on EPAPS, see http://www.aip.org/pubservs/epaps. html.
[17] S. N. Kale *et al.*, Appl. Phys. Lett. **82**, 2100 (2003).
[18] H. Raebiger *et al.*, J. Magn. Magn. Mater. **290**, 1398 (2005).
[19] H. Raebiger, A. Ayuela, and J. von Boehm, Phys. Rev. B **72**, 014465 (2005).
[20] S. Kuroda *et al.*, Nat. Mater. **6**, 440 (2007); N. Samarth, *ibid.* **6**403 (2007).
[21] G. Kresse and J. Furthmüller, Phys. Rev. B **54**, 11 169 (1996); G. Kresse and D. Joubert, *ibid.* **59**, 1758 (1999).
[22] H. Raebiger, S. Lany, and A. Zunger, Phys. Rev. B, **76**, 045209 (2007).
[23] We determine the shift of the VBM by calculating the VBM with respect to the average potential within GGA + U (with U = 6 and J = 1 eV), and find that the VBM shifts down by −0.32 eV when on site Coulomb correction is included. The remaining discrepancy with the experimental gap is recovered by a rigid shift of the CBM.
[24] C. Persson *et al.*, Phys. Rev. B **72**, 035211 (2005).
[25] J. Osorio-Guillén *et al.*, Phys. Rev. Lett. **96**, 107203 (2006).
[26] M. Sieberer, J. Redinger, and P. Mohn, Phys. Rev. B **75**, 035203 (2007).
[27] A. F. Wright and J. S. Nelson, J. Appl. Phys. **92**, 5849 (2002).
[28] H. Raebiger, M. G. Ganchenkova, and J. von Boehm, Appl. Phys. Lett. **89**, 012505 (2006).